



## OPEN ACCESS

## EDITED BY

Levon Abrahamyan,  
Montreal University, Canada

## REVIEWED BY

Dimitra K. Toubanaki,  
Pasteur Hellenic Institute, Greece  
Carlos Llorens,  
Biotechvana SL, Spain

## \*CORRESPONDENCE

Julia Béjar  
✉ bejar@uma.es  
Ana Grande-Pérez  
✉ agrande@uma.es

<sup>†</sup>These authors share first authorship

RECEIVED 09 March 2023

ACCEPTED 23 May 2023

PUBLISHED 15 June 2023

## CITATION

Ortega-del Campo S, Díaz-Martínez L,  
Moreno P, García-Rosado E, Alonso MC,  
Béjar J and Grande-Pérez A (2023) The genetic  
variability and evolution of red-spotted grouper  
nervous necrosis virus quasispecies can  
be associated with its virulence.  
*Front. Microbiol.* 14:1182695.  
doi: 10.3389/fmicb.2023.1182695

## COPYRIGHT

© 2023 Ortega-del Campo, Díaz-Martínez,  
Moreno, García-Rosado, Alonso, Béjar and  
Grande-Pérez. This is an open-access article  
distributed under the terms of the [Creative Commons Attribution License \(CC BY\)](https://creativecommons.org/licenses/by/4.0/). The  
use, distribution or reproduction in other  
forums is permitted, provided the original  
author(s) and the copyright owner(s) are  
credited and that the original publication in this  
journal is cited, in accordance with accepted  
academic practice. No use, distribution or  
reproduction is permitted which does not  
comply with these terms.

# The genetic variability and evolution of red-spotted grouper nervous necrosis virus quasispecies can be associated with its virulence

Sergio Ortega-del Campo<sup>1†</sup>, Luis Díaz-Martínez<sup>2†</sup>,  
Patricia Moreno<sup>3,4</sup>, Esther García-Rosado<sup>3,4</sup>, M. Carmen Alonso<sup>3,4</sup>,  
Julia Béjar<sup>1,4\*</sup> and Ana Grande-Pérez<sup>1,5\*</sup>

<sup>1</sup>Departamento de Biología Celular, Genética y Fisiología, Facultad de Ciencias, Universidad de Málaga, Málaga, Spain, <sup>2</sup>Centro de Supercomputación y Bioinnovación (SCBI), Universidad de Málaga, Málaga, Spain, <sup>3</sup>Departamento de Microbiología, Facultad de Ciencias, Universidad de Málaga, Málaga, Spain, <sup>4</sup>Instituto de Biotecnología y Desarrollo Azul, IBYDA, Universidad de Málaga, Málaga, Spain, <sup>5</sup>Instituto de Hortofruticultura Subtropical y Mediterránea "La Mayora", Universidad de Málaga- Consejo Superior de Investigaciones Científicas (IHSM-UMA-CSIC), Málaga, Spain

Nervous necrosis virus, NNV, is a neurotropic virus that causes viral nervous necrosis disease in a wide range of fish species, including European sea bass (*Dicentrarchus labrax*). NNV has a bisegmented (+) ssRNA genome consisting of RNA1, which encodes the RNA polymerase, and RNA2, encoding the capsid protein. The most prevalent NNV species in sea bass is red-spotted grouper nervous necrosis virus (RGNNV), causing high mortality in larvae and juveniles. Reverse genetics studies have associated amino acid 270 of the RGNNV capsid protein with RGNNV virulence in sea bass. NNV infection generates quasispecies and reassortants able to adapt to various selective pressures, such as host immune response or switching between host species. To better understand the variability of RGNNV populations and their association with RGNNV virulence, sea bass specimens were infected with two RGNNV recombinant viruses, a wild-type, rDI956, highly virulent to sea bass, and a single-mutant virus, Mut270DI965, less virulent to this host. Both viral genome segments were quantified in brain by RT-qPCR, and genetic variability of whole-genome quasispecies was studied by Next Generation Sequencing (NGS). Copies of RNA1 and RNA2 in brains of fish infected with the low virulent virus were 1,000-fold lower than those in brains of fish infected with the virulent virus. In addition, differences between the two experimental groups in the Ts/Tv ratio, recombination frequency and genetic heterogeneity of the mutant spectra in the RNA2 segment were found. These results show that the entire quasispecies of a bisegmented RNA virus changes as a consequence of a single point mutation in the consensus sequence of one of its segments. Sea bream (*Sparus aurata*) is an asymptomatic carrier for RGNNV, thus rDI965 is considered a low-virulence isolate in this species. To assess whether the quasispecies characteristics of rDI965 were conserved in another host showing different susceptibility, juvenile sea bream were infected with rDI965 and analyzed as above described. Interestingly, both viral load and genetic variability of rDI965 in seabream were similar to those of Mut270DI965 in sea bass. This result suggests that the genetic variability and evolution of RGNNV mutant spectra may be associated with its virulence.

## KEYWORDS

NNV, virulence, quasispecies, NGS, genetic variability, haplotype reconstruction, recombination, comparative analysis

## 1. Introduction

Aquaculture is an increasingly important activity, with a major global economic impact. The main constraint to aquaculture development is the occurrence of infectious disease outbreaks. Furthermore, the rapid growth of aquaculture, intensive farming techniques, introduction of new species and the environmental change provide ideal conditions for the emergence of new pathogens (Pérez-Sánchez et al., 2018).

Nervous necrosis virus (NNV), belonging to the *Betanodavirus* genus (*Nodaviridae* family), is one of the most harmful pathogens to the aquaculture industry, causing viral nervous necrosis (VNN), also known as viral encephalopathy and retinopathy (VER), a severe disease affecting the central nervous system (CNS) of numerous marine and freshwater fish species worldwide (Thiéry et al., 2004; Kara et al., 2014; Doan et al., 2017; Bandín and Souto, 2020). VER particularly affects hatchery-reared larvae and juveniles, causing high mortality rate (80–100%) (Le Breton et al., 1997; Munday et al., 2002; Volpe et al., 2020).

NNV genome consists of two single-stranded RNA molecules of positive polarity (+ ssRNA), RNA1 and RNA2. RNA1 (3.1 kb) contains a single open reading frame (ORF) that encodes an RNA-dependent RNA polymerase (RdRp), also known as protein A, whereas RNA2 (1.4 kb) encodes the capsid protein (Cp) (Munday et al., 2002; Chen et al., 2015; Bandín and Souto, 2020). Replication of the viral genome involves a subgenomic RNA (sgRNA3, 371–378 nt), transcribed from the 3' end of the RNA1 segment, that encodes two non-structural proteins, B1 and B2 (Iwamoto et al., 2001; Bandín and Souto, 2020).

There are four NNV species based on RNA2 sequencing: barfin flounder nervous necrosis virus (BFNNV), red-spotted grouper nervous necrosis virus (RGNNV), striped jack nervous necrosis virus (SJNNV), and tiger puffer nervous necrosis virus (TPNNV) (Nishizawa et al., 1997). The main NNV reported in the Mediterranean area are RGNNV and SJNNV, which affect European sea bass (*Dicentrarchus labrax*) and sea bream (*Sparus aurata*). Moreover, RGNNV-SJNNV reassortant isolates, presenting both segment combinations, SJNNV/RGNNV and RGNNV/SJNNV (RNA1/RNA2), have been isolated from several fish species (Toffolo et al., 2007; Oliveira et al., 2009; Toffan et al., 2017; Qin et al., 2020; Volpe et al., 2020). Specifically, European sea bass is highly susceptible to RGNNV infections, whereas sea bream is resistant to RGNNV but susceptible to SJNNV and RGNNV/SJNNV infections (Castric et al., 2001; Oliveira et al., 2009; Chaves-Pozo et al., 2012; Vendramin et al., 2014; Souto et al., 2015b; Carballo et al., 2016; Toffan et al., 2017; Volpe et al., 2020; Pereiro et al., 2023).

The fitness of NNV in its hosts is determined by a high genetic diversity, with reassortment as one of the main sources of genetic diversity (Panzarin et al., 2016). Furthermore, reassortment has been associated

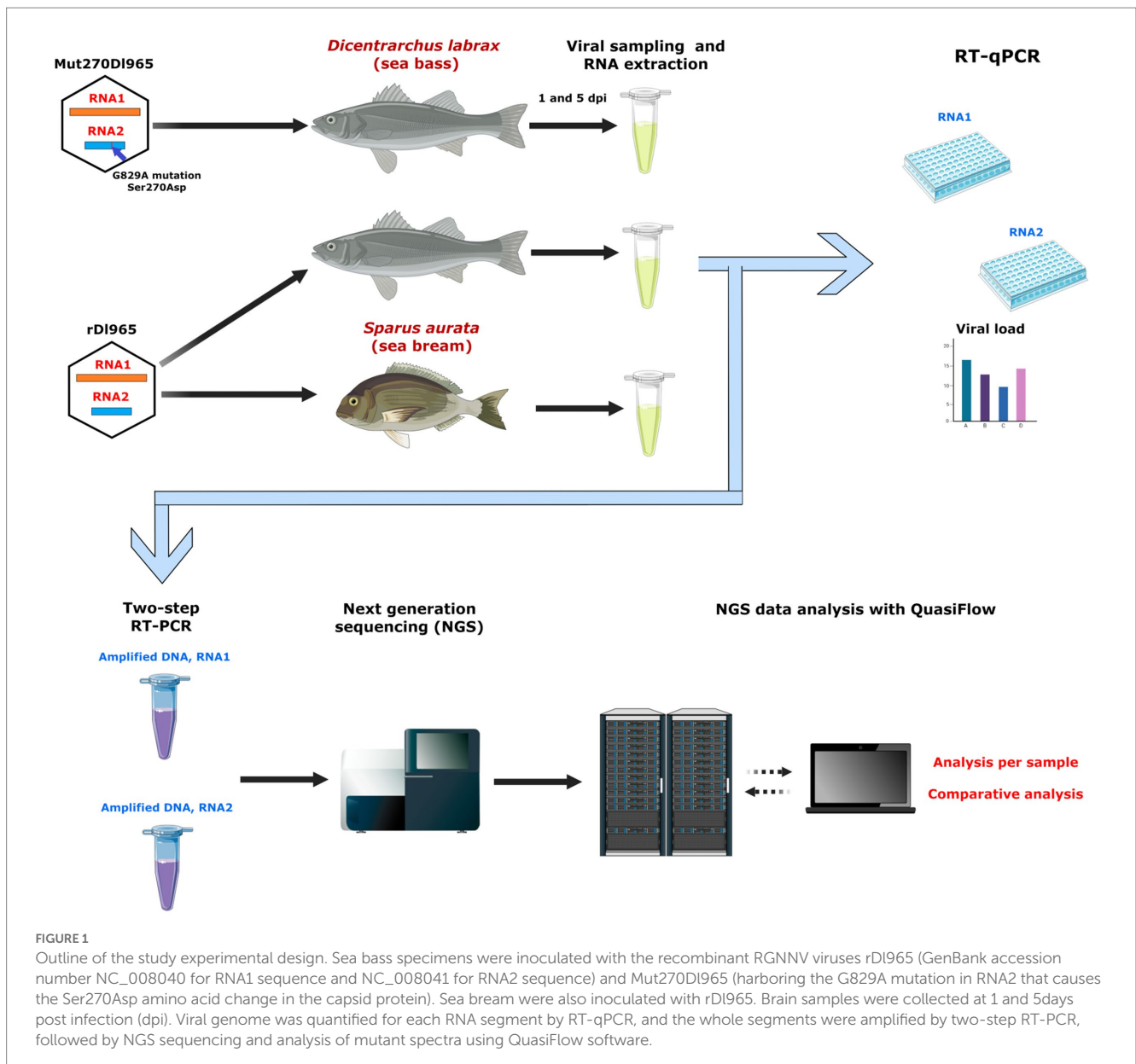
with colonization of new fish species. Several studies have shown that both sea bream and sea bass are susceptible to RGNNV/SJNNV, although it has been suggested that sea bass could act as a reservoir, since a high viral load has been detected in asymptomatic specimens (Biasini et al., 2022). As RNA viruses, NNV possess high mutation rates that, along with their small genomic size, result in mutant spectra characterized by high variability and genetic heterogeneity (Sugaya et al., 2009; Panzarin et al., 2012). Although NNV genetic variation has been poorly examined, several studies have shown that NNV is organized as quasispecies (Hick et al., 2010; Chen et al., 2020).

The role of quasispecies in RGNNV virulence *in vivo* has been analyzed in the present study (experimental design shown in Figure 1). To that aim, two viruses that had been obtained by reverse genetics in a previous study were used, namely a recombinant RGNNV (rDI965), causing 73.3% mortality in sea bass, and an attenuated RGNNV (Mut270DI965), with 20% mortality in sea bass (Moreno et al., 2019). Mut270DI965 had a non-synonymous mutation at position 270 of the Cp protein, which produces a serine to asparagine amino acid change. Whole genome mutant spectra were analyzed by New Generation Sequencing (NGS), genetic variability and diversity were estimated, haplotypes composing the mutant spectra of both genomic segments were reconstructed, and a statistical comparison of all samples was performed. According to our results, the presence of the non-synonymous mutation at position 270 of the Cp protein, which is a virulence determinant of RGNNV in sea bass, leads to a change in the genetic quasispecies variability. To evaluate whether the quasispecies characteristics of rDI965, highly virulent to sea bass, were conserved in a different host showing low susceptibility, sea bream juveniles were also infected with rDI965. Interestingly, results showed that rDI965 quasispecies in sea bream are similar to Mut270DI965 quasispecies in sea bass.

## 2. Materials and methods

### 2.1. Virus and cell culture

The recombinant rDI965 virus had been generated by reverse genetics from the RGNNV isolate SpDI\_IAusc965.09, obtained from a diseased European sea bass (Moreno et al., 2019). Mut270DI965, derived from rDI965, carries a site-specific mutation at position 830 within the RNA2 segment (aa270 of the Cp sequence, Ser270Asp) (Moreno et al., 2019). Both recombinant viruses were propagated using the E11 cell line (Iwamoto et al., 2001), at 25°C, with Leibovitz L-15 medium (Gibco) supplemented with 2% foetal bovine serum (FBS, Gibco), 100 units/mL penicillin and 10 mg/mL streptomycin (Sigma) until complete cytopathic effects (CPE) were observed. The resulting viral suspension was titrated following the 50% tissue culture infective dose method (TCID<sub>50</sub>) (Reed and Muench, 1938) and stored at –80°C until used.



## 2.2. European sea bass and sea bream challenge

Juvenile sea bass (8g, average weight) were distributed into 3 experimental groups ( $n=20$ ): (i) rDI965-infected group, (ii) Mut270DI965-infected group, and (iii) L-15-injected group, as negative control. Specimens were infected intramuscularly at a dose of  $2 \times 10^6$  TCID<sub>50</sub>/fish. Juvenile sea bream specimens (8g, average weight) were only injected with rDI965 ( $2 \times 10^6$  TCID<sub>50</sub>/fish). At 1 and 5 days post-injection (dpi), three animals per group were sacrificed by MS-22 overdose, and brains were individually collected and stored in liquid nitrogen for subsequent analyses (Table 1).

## 2.3. Ethics statement

Fish were always handled according to the European Union guidelines for the handling of laboratory animals (Directive 2010/63/

UE), applying the lowest stress-generating conditions of light, oxygen and feeding. To minimize fish suffering, trials were accomplished in accordance with the Bioethics Committee of Junta de Andalucía (number: 09/08/2019/136).

## 2.4. RNA extraction, amplification, and next-generation sequencing

Total RNA was extracted from brain using TRI reagent solution, quantified using the NanoDrop ND 1000 microdrop spectrophotometer system (Thermo Fisher), and diluted to 800 ng/ $\mu$ l. cDNA synthesis was performed in duplicate using AMV RT (Promega), with 1 mM dNTP, 0.4  $\mu$ M reverse primer (3'R1\_965 for RNA1 and 3'R2\_965 for RNA2), 4 u/ $\mu$ l RNasin Ribonuclease Inhibitor, 352 ng/ $\mu$ l RNA and 30 u AMV RT. The maximum volume of RNA was added to the reaction to avoid bottlenecks and loss of low-frequency haplotypes of the viral quasispecies. After

TABLE 1 Samples analyzed in this study, organized by host species, days post-infection (dpi), and viruses inoculated.

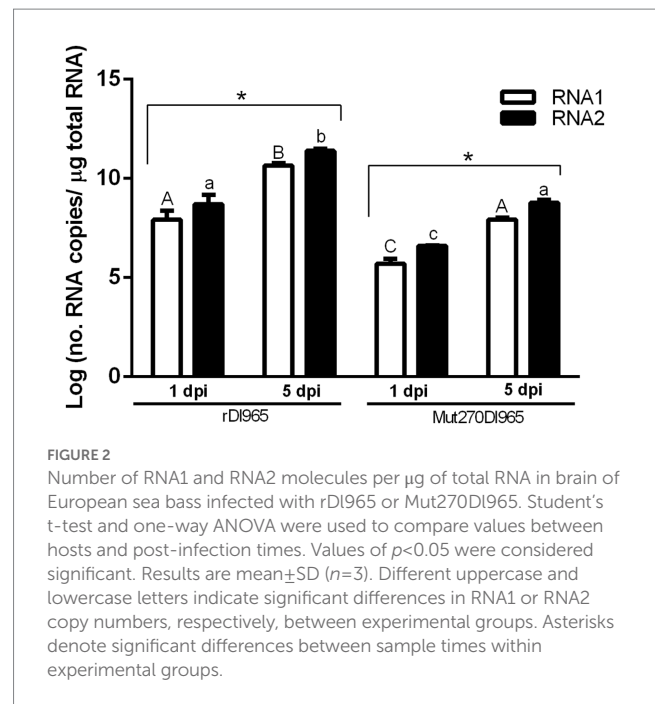
Virus	dpi	Host	
		<i>Dicentrarchus labrax</i>	<i>Sparus aurata</i>
rDI965	1	Dla_WT_1_r1	Sau_WT_1_r1
		Dla_WT_1_r2	Sau_WT_1_r2
		Dla_WT_1_r3	Sau_WT_1_r3
	5	Dla_WT_5_r1	Sau_WT_5_r1
		Dla_WT_5_r2	Sau_WT_5_r2
		Dla_WT_5_r3	Sau_WT_5_r3
Mut270DI965	1	Dla_Mut_1_r1	
		Dla_Mut_1_r2	
		Dla_Mut_1_r3	
	5	Dla_Mut_5_r1	
		Dla_Mut_5_r2	
		Dla_Mut_5_r3	

incubation at 42°C for 60 min, duplicate RT reactions were mixed and cDNA was quantified. Duplicate PCR reactions for each genomic segment were performed using 0.25 mM dNTP, 0.2 μM specific primers (T7\_5'R1\_965/3'R1\_965 for RNA1, and T7\_5'R2\_965/3'R2\_965 for RNA2) (Supplementary material S1), 4–8 ng of cDNA and 40 u *PfuUltra* II Fusion HS DNA polymerase (Agilent). Amplification reaction was carried out according to the manufacturer's instructions, including an initial denaturation cycle of 1 min at 95°C, followed by 30 cycles of 20 s at 95°C for denaturation, 20 s at 55°C for annealing and 2 min at 72°C for elongation. A final elongation cycle at 72°C for 3 min was included as a final step. As a result, two amplicons were obtained, corresponding to RNA1 and RNA2 viral segments. Duplicate PCR products of each genomic segment per sample were pooled prior to sequencing.

DNA library was prepared using the Nextera XT DNA Library Prep Kit (Illumina), according to the manufacturer's protocol. Briefly, PCR products were subjected to tagmentation, which enzymatically cleaved and tagged DNA with Illumina adapters. DNA was then subjected to a 12-cycle PCR, for indexing/barcoding, with a unique combination of 15 and 17 index primers. Amplification products were purified using Agencourt AMPure XP beads (Beckman Coulter Inc., CA, USA) and manually normalized. High-throughput sequencing was performed with Nextseq 550 Reagent Mid Output Kit v2.5 (300-cycle, Illumina) to generate 3–10 million 150-nucleotide paired-end reads per sequencing run, using the proprietary Illumina Nextseq550 System. DNA library preparation and sequencing were performed at the Supercomputing and Bioinnovation Center (SCBI) of the University of Malaga (Spain).

## 2.5. Viral genome quantification

RNA1 and RNA2 quantification was performed by absolute RT-qPCR following the procedure described by Moreno et al. (2016, 2019). Specific pairs of primers for RNA1 and RNA2 amplification were RG-RNA1-F/RG-RNA1-R (Lopez-Jimena et al., 2011), and



RG\_965\_RNA2 F4/RG\_965\_RNA2 R1 (Moreno et al., 2016), respectively. RNA was purified from rDI965 ( $10^7$  TCID<sub>50</sub>/ml), quantified by DS-11 Fx+ (Denovix), and diluted to be used as a reference standard curve. RNA was reverse transcribed using AMV reverse transcriptase (Promega). Significant differences in viral load between sea bass samples infected with rDI965 or Mut270DI965, as well as between sea bass and sea bream samples infected with rDI965, were tested by Student's t-tests and one-way ANOVA. Statistical analyses were performed using GraphPad software (Figure 2; Figure 5).

## 2.6. Genetic variability of quasispecies

The genetic complexity and heterogeneity of RGNNV-mutant spectra were analyzed using QuasiFlow, an open-source workflow for the analysis of viral quasispecies using NGS data (Seoane et al., 2022). QuasiFlow was run on PICASSO supercomputer (SCBI, University of Malaga, Spain). QuasiFlow analyses were performed separately for each viral segment (RNA1 and RNA2). The analyses were performed using the default conditions.

The composition and distribution of mutations (SNPs, InDels) was firstly obtained. We analyzed possible biases in the types of substitutions per group of samples, classified by time of sampling, virus and host. The expected frequency for a given substitution (substitution of nt X by nt Y,  $f_{E X \rightarrow Y}$ ) was calculated assuming that all substitutions were equally likely following this formula:

$$f_{E X \rightarrow Y} = \frac{P_x * M}{3}$$

$P_x$  = fractional proportion of nucleotides X (= A, G, T or C) in parental sequence.

M = total mutations observed.

Significant deviations of the expected number of each substitution were tested using a  $2 \times 2$  chi-square test.

Mutation frequency was calculated as the proportion of mutated residues in the alignment compared to the reference sequence (Seoane et al., 2022). Nucleotide diversity, measured as the average number of nucleotide differences between any two genomes of the quasispecies (Gregori et al., 2016), was also estimated. Haplotypes were reconstructed and quasispecies heterogeneity was analyzed using the normalized Shannon index, i.e., a measure of diversity based on haplotype frequencies (Gregori et al., 2016). The workflow established an iterative analysis of the reads, joining them if they are identical within 90% of their length creating haplotypes. In this way, the reads cycle by cycle decreased in number, and increased in nucleotide length until all possible haplotypes were generated. Once each haplotype was reconstructed, and the variations of each mutant spectrum were identified, the viral quasispecies were represented by networks connecting haplotypes with their mutations (SNPs and InDels) (Seoane et al., 2022).

Recombination events, as well as breakpoints in genome segments, were detected for each sample. Recombination frequency, that is, the number of recombinant reads divided by the total number of reads analyzed, was also estimated (Gregori et al., 2016; Seoane et al., 2022).

Comparative analyses between samples were performed using the QuasiComparer workflow (Seoane et al., 2022). Statistical analyses included ANOVA for comparative analysis between samples or sample variables (host species, dpi, rDI965 or Mut270DI965), Shannon index and nucleotide diversity, calculated from reconstructed haplotypes, and principal component analysis (PCA) of all samples with all variables considered (Seoane et al., 2022).

## 3. Results

### 3.1. Viral genome quantification

Viral load in the brain of sea bass was tested in each experimental group by absolute RT-qPCR. Viral RNA1 and RNA2 were not detected in the negative control group, whereas in the groups infected with rDI965 or Mut270DI965 they were quantified at the two sampling times considered (Figure 2; Supplementary material S2). RNA2 was more abundant than RNA1 in all samples, although the differences were not significant. The number of RNA1 and RNA2 copies of both viruses significantly increased from 1 to 5 dpi ( $p < 0.0001$ ), reaching at the latter sampling time the maximum mean value of genome copies observed for both RNA1 (10.65 and 7.93 log copies/ $\mu$ g RNA for rDI965 and Mut270DI965, respectively) and RNA2 (11.39 and 8.78 log copies/ $\mu$ g RNA, for rDI965 and Mut270DI965, respectively). Moreover, the mean values obtained for RNA1 and RNA2 copy number in Mut270DI965 were significantly lower than those obtained for the non-mutated virus at 5 dpi ( $p < 0.0001$ ).

### 3.2. Genetic complexity of viral quasispecies in sea bass

Quasispecies characterization was firstly approached through analysis of individual samples (QuasiFlow analysis). After sequence filtering, between  $6.87 \times 10^5$  and  $5.99 \times 10^6$  paired reads per sample, and coverage between  $2.69 \times 10^4$  and  $5.50 \times 10^5$  nucleotides per nucleotide position, were obtained (Table 2; Supplementary material S3).

We firstly analyzed the composition of mutations within RGNNV populations from sea bass, focusing on detecting possible point mutation biases. We observed a bias in base substitutions in the set of mutant spectra related to transition mutations. An overrepresentation of transitions was detected in all samples, in both segments, showing a Ts/Tv ratio between 3.68 and 16.21 (Table 2; Supplementary materials S3, S4), with high statistical significance ( $p < 0.01$ ) (Supplementary material S5). The weight of transitions was not uniform in all samples. The abundance of transitions in the genome increased over time. However, there was a downward trend in the weight of transitions in Mut270DI965 samples. Overall, Ts/Tv ratio was significantly lower in Mut270DI965 than in rDI965 samples, especially at 1 dpi (Supplementary material S3). The lower Ts/Tv values were due to a considerable reduction in the number of T  $\rightarrow$  C and C  $\rightarrow$  T transitions (Supplementary materials S4, S5).

The complexity of RGNNV quasispecies was measured by estimates of mutation frequency and nucleotide diversity. Mutation frequency values ranged from  $4.30 \times 10^{-4}$  to  $2.97 \times 10^{-3}$  mut/nt in RNA1 and from  $1.35 \times 10^{-3}$  to  $1.06 \times 10^{-2}$  mut/nt in RNA2. Overall, mutation frequency values in Mut270DI965 populations were significantly different from those in rDI965 populations, although with significant differences between viral segments. In virulent virus (rDI965) samples, there was a significant increase in mutation frequency in the RNA1 segment from 1 dpi ( $4.30\text{--}4.43 \times 10^{-4}$  mut/nt) to 5 dpi ( $5.37 \times 10^{-4}\text{--}1.99 \times 10^{-3}$  mut/nt). However, in low virulence virus (Mut270DI965) samples, this parameter remained constant overtime, although a downward trend was detected at 5 dpi. Thus, rDI965 quasispecies were more complex at 5 dpi, whereas Mut270DI965 complexity remained constant or even declined. In contrast, from 1 to 5 dpi, a decrease in genetic complexity was detected in RNA2 rDI965 quasispecies in sea bass. Mutation frequency ranged from  $1.92 \times 10^{-3}$  to  $7.22 \times 10^{-3}$  mut/nt at 1 dpi, dropping to values too low to be quantified by the workflow at 5 dpi (Table 2; Supplementary material S3). However, Mut270DI965 RNA2 mutation frequency was the same at 1 dpi ( $1.35\text{--}1.75 \times 10^{-3}$  mut/nt) as at 5 dpi ( $1.93 \times 10^{-3}\text{--}1.06 \times 10^{-2}$  mut/nt) (Table 2; Supplementary material S3). Thus, the less virulent Mut270DI965 virus quasispecies showed much greater genetic complexity in RNA2 than the virulent rDI965 virus quasispecies at 5 dpi.

The same patterns were observed when estimating genetic diversity. In the rDI965 samples, the RNA1 nucleotide diversity increased over time ( $8.59\text{--}8.86 \times 10^{-4}$  and  $1.07\text{--}3.95 \times 10^{-3}$  at 1 and 5 dpi, respectively). However, RNA2 diversity decreased in samples collected at 5 dpi. Conversely, Mut270DI965 nucleotide diversity remained constant for both segments at 1 and 5 dpi (Table 2; Supplementary material S3).

### 3.3. Recombination analysis in sea bass samples

Using the QuasiFlow tool, recombinant viruses were detected in the mutant spectra, and the recombination frequency was estimated (Seoane et al., 2022). The recombination frequency was different for each genomic segment. Thus, the estimated recombination frequency for RNA1 for all samples ranged from  $10^{-2}$  to  $10^{-1}$  recombinant reads per total number of reads (rec/rd), a wider range than that recorded for RNA2 ( $10^{-4}\text{--}10^{-2}$  rec/rd). In general, the recombination events

TABLE 2 Genetic complexity and heterogeneity values obtained for each of the RGNV samples in each genomic segment.

RNA segment	Sample	Coverage	Mutation frequency <sup>a</sup>	H <sub>n</sub> <sup>b</sup>	H <sub>SN</sub> <sup>c</sup>	Nucleotide diversity	Recombination frequency <sup>d</sup>
RNA1	Dla_WT_1_r1	1.83 × 10 <sup>5</sup>	4.30 × 10 <sup>-4</sup>	3	0.04	8.59 × 10 <sup>-4</sup>	7.51 × 10 <sup>-2</sup>
	Dla_WT_1_r2	1.83 × 10 <sup>5</sup>	4.43 × 10 <sup>-4</sup>	8	0.23	8.86 × 10 <sup>-4</sup>	3.46 × 10 <sup>-2</sup>
	Dla_WT_1_r3	1.22 × 10 <sup>5</sup>	-	-	0	-	5.32 × 10 <sup>-2</sup>
	Dla_WT_5_r1	1.59 × 10 <sup>5</sup>	1.99 × 10 <sup>-3</sup>	16	0.1	3.95 × 10 <sup>-3</sup>	1.63 × 10 <sup>-2</sup>
	Dla_WT_5_r2	2.17 × 10 <sup>5</sup>	7.79 × 10 <sup>-4</sup>	12	0.12	1.53 × 10 <sup>-3</sup>	2.03 × 10 <sup>-2</sup>
	Dla_WT_5_r3	2.04 × 10 <sup>5</sup>	5.37 × 10 <sup>-4</sup>	6	0.32	1.07 × 10 <sup>-3</sup>	2.06 × 10 <sup>-2</sup>
	Dla_Mut_1_r1	5.11 × 10 <sup>4</sup>	5.64 × 10 <sup>-4</sup>	8	0.22	1.13 × 10 <sup>-3</sup>	3.66 × 10 <sup>-2</sup>
	Dla_Mut_1_r2	2.69 × 10 <sup>4</sup>	2.97 × 10 <sup>-3</sup>	9	0.31	5.46 × 10 <sup>-3</sup>	1.61 × 10 <sup>-2</sup>
	Dla_Mut_1_r3	3.63 × 10 <sup>4</sup>	6.69 × 10 <sup>-4</sup>	13	0.11	1.31 × 10 <sup>-3</sup>	-
	Dla_Mut_5_r1	1.94 × 10 <sup>5</sup>	5.86 × 10 <sup>-4</sup>	11	0.37	1.14 × 10 <sup>-3</sup>	9.75 × 10 <sup>-2</sup>
	Dla_Mut_5_r2	1.91 × 10 <sup>5</sup>	1.02 × 10 <sup>-3</sup>	6	0.1	1.35 × 10 <sup>-3</sup>	8.81 × 10 <sup>-2</sup>
	Dla_Mut_5_r3	1.77 × 10 <sup>5</sup>	4.30 × 10 <sup>-4</sup>	6	0.43	8.59 × 10 <sup>-4</sup>	1.42 × 10 <sup>-1</sup>
	Sau_WT_1_r1	4.46 × 10 <sup>4</sup>	6.44 × 10 <sup>-4</sup>	18	0.04	1.28 × 10 <sup>-3</sup>	1.83 × 10 <sup>-2</sup>
	Sau_WT_1_r2	1.85 × 10 <sup>5</sup>	1.43 × 10 <sup>-3</sup>	9	0.06	2.86 × 10 <sup>-3</sup>	3.23 × 10 <sup>-2</sup>
	Sau_WT_1_r3	3.12 × 10 <sup>4</sup>	7.16 × 10 <sup>-4</sup>	9	0.1	1.41 × 10 <sup>-3</sup>	2.80 × 10 <sup>-2</sup>
	Sau_WT_5_r1	1.70 × 10 <sup>5</sup>	1.66 × 10 <sup>-3</sup>	7	0.36	3.28 × 10 <sup>-3</sup>	4.41 × 10 <sup>-2</sup>
	Sau_WT_5_r2	1.38 × 10 <sup>5</sup>	1.20 × 10 <sup>-3</sup>	7	0.42	2.39 × 10 <sup>-3</sup>	4.98 × 10 <sup>-2</sup>
	Sau_WT_5_r3	1.56 × 10 <sup>5</sup>	7.25 × 10 <sup>-4</sup>	12	0.08	1.45 × 10 <sup>-3</sup>	5.68 × 10 <sup>-2</sup>
RNA2	Dla_WT_1_r1	4.63 × 10 <sup>5</sup>	1.92 × 10 <sup>-3</sup>	4	0.01	3.84 × 10 <sup>-3</sup>	5.15 × 10 <sup>-3</sup>
	Dla_WT_1_r2	4.60 × 10 <sup>5</sup>	6.46 × 10 <sup>-3</sup>	4	0.08	1.29 × 10 <sup>-2</sup>	1.52 × 10 <sup>-2</sup>
	Dla_WT_1_r3	5.50 × 10 <sup>5</sup>	7.22 × 10 <sup>-3</sup>	3	0.02	1.44 × 10 <sup>-2</sup>	8.74 × 10 <sup>-3</sup>
	Dla_WT_5_r1	4.89 × 10 <sup>5</sup>	-	-	-	-	9.03 × 10 <sup>-3</sup>
	Dla_WT_5_r2	4.59 × 10 <sup>5</sup>	-	-	-	-	2.08 × 10 <sup>-2</sup>
	Dla_WT_5_r3	5.26 × 10 <sup>5</sup>	-	-	-	-	1.14 × 10 <sup>-2</sup>
	Dla_Mut_1_r1	3.86 × 10 <sup>5</sup>	1.75 × 10 <sup>-3</sup>	18	0.27	3.32 × 10 <sup>-3</sup>	-
	Dla_Mut_1_r2	4.87 × 10 <sup>5</sup>	1.35 × 10 <sup>-3</sup>	14	0.03	2.68 × 10 <sup>-3</sup>	1.06 × 10 <sup>-4</sup>
	Dla_Mut_1_r3	2.79 × 10 <sup>5</sup>	1.40 × 10 <sup>-3</sup>	10	0.04	2.76 × 10 <sup>-3</sup>	3.48 × 10 <sup>-4</sup>
	Dla_Mut_5_r1	2.02 × 10 <sup>5</sup>	1.93 × 10 <sup>-3</sup>	13	0.04	3.74 × 10 <sup>-3</sup>	1.40 × 10 <sup>-4</sup>
	Dla_Mut_5_r2	5.30 × 10 <sup>5</sup>	1.06 × 10 <sup>-2</sup>	4	0.06	2.13 × 10 <sup>-2</sup>	1.09 × 10 <sup>-4</sup>
	Dla_Mut_5_r3	4.25 × 10 <sup>5</sup>	-	-	-	-	5.84 × 10 <sup>-3</sup>
	Sau_WT_1_r1	3.19 × 10 <sup>5</sup>	1.62 × 10 <sup>-2</sup>	4	0.06	1.80 × 10 <sup>-2</sup>	2.58 × 10 <sup>-2</sup>
	Sau_WT_1_r2	2.89 × 10 <sup>5</sup>	3.21 × 10 <sup>-3</sup>	5	0.03	6.28 × 10 <sup>-3</sup>	8.92 × 10 <sup>-3</sup>
	Sau_WT_1_r3	3.66 × 10 <sup>5</sup>	1.55 × 10 <sup>-3</sup>	9	0.11	3.06 × 10 <sup>-3</sup>	2.41 × 10 <sup>-3</sup>
	Sau_WT_5_r1	5.79 × 10 <sup>5</sup>	1.14 × 10 <sup>-2</sup>	3	0.03	2.23 × 10 <sup>-2</sup>	2.21 × 10 <sup>-3</sup>
	Sau_WT_5_r2	5.55 × 10 <sup>5</sup>	-	-	-	-	1.70 × 10 <sup>-3</sup>
	Sau_WT_5_r3	6.00 × 10 <sup>5</sup>	9.54 × 10 <sup>-3</sup>	3	0.02	1.91 × 10 <sup>-2</sup>	2.36 × 10 <sup>-4</sup>

<sup>a</sup>Mutation frequency (proportion of mutant nucleotides in a population) measured in mut/nt. <sup>b</sup>Number of haplotypes. <sup>c</sup>Normalized Shannon Index. <sup>d</sup>Recombination frequency, expressed as number of recombinant reads divided by total number of reads (rec/rd).

detected were homologous. Non-homologous recombination events were less abundant, being present mainly in rDI965-infected samples (Supplementary material S3).

Significant differences between the high virulent (rDI965) and low virulent quasispecies (Mut270DI965) were detected in sea bass. Regarding RNA1, the recombination frequency in Mut270DI965 populations was significantly higher ( $p < 0.01$ ) than in rDI965 populations at 5 dpi

( $1.63\text{--}2.06 \times 10^{-2}$  rec/rd for rDI965, and  $8.81 \times 10^{-2}\text{--}1.42 \times 10^{-1}$  for Mut270DI965) (Table 2; Supplementary material S3). According to our results, a decrease in the generation of recombination events in RNA1 was observed from 1 to 5 dpi in the virulent quasispecies, whereas the number of recombinants increased considerably in the low virulent quasispecies in the same time interval. Regarding RNA2, virulent quasispecies underwent more recombination events than the less virulent quasispecies

over time ( $p < 0.01$ ). Recombination frequency in rDI965 samples was significantly higher ( $5.15 \times 10^{-3}$ – $1.52 \times 10^{-2}$  rec/rd at 1 dpi and  $9.03 \times 10^{-3}$ – $2.08 \times 10^{-2}$  rec/rd at 5 dpi) than in Mut270DI965 samples ( $1.06$ – $3.48 \times 10^{-4}$  rec/rd and  $1.40 \times 10^{-4}$ – $1.09 \times 10^{-2}$  rec/rd at 1 and 5 dpi, respectively) (Table 2; Supplementary material S3).

In addition, very characteristic recombination patterns between 3' and 5' ends of the RNA1 segment were observed (Figure 3; Supplementary material S6). Specifically, recombination originated in the region between nucleotide positions 2,850–3,050 and the region between positions 150–350. Nucleotide base coverage showed a characteristic pattern that could be correlated with recombination events, as it was significantly higher at 5' and 3' ends than in the rest of the genome. At some positions, coincident with recombination breakpoints, the coverage reached  $10^6$  reads/base, i.e., ten-times higher than the average coverage estimated for the whole genome. Conversely, in the RNA2 segment, no recombination patterns common at all samples were detected.

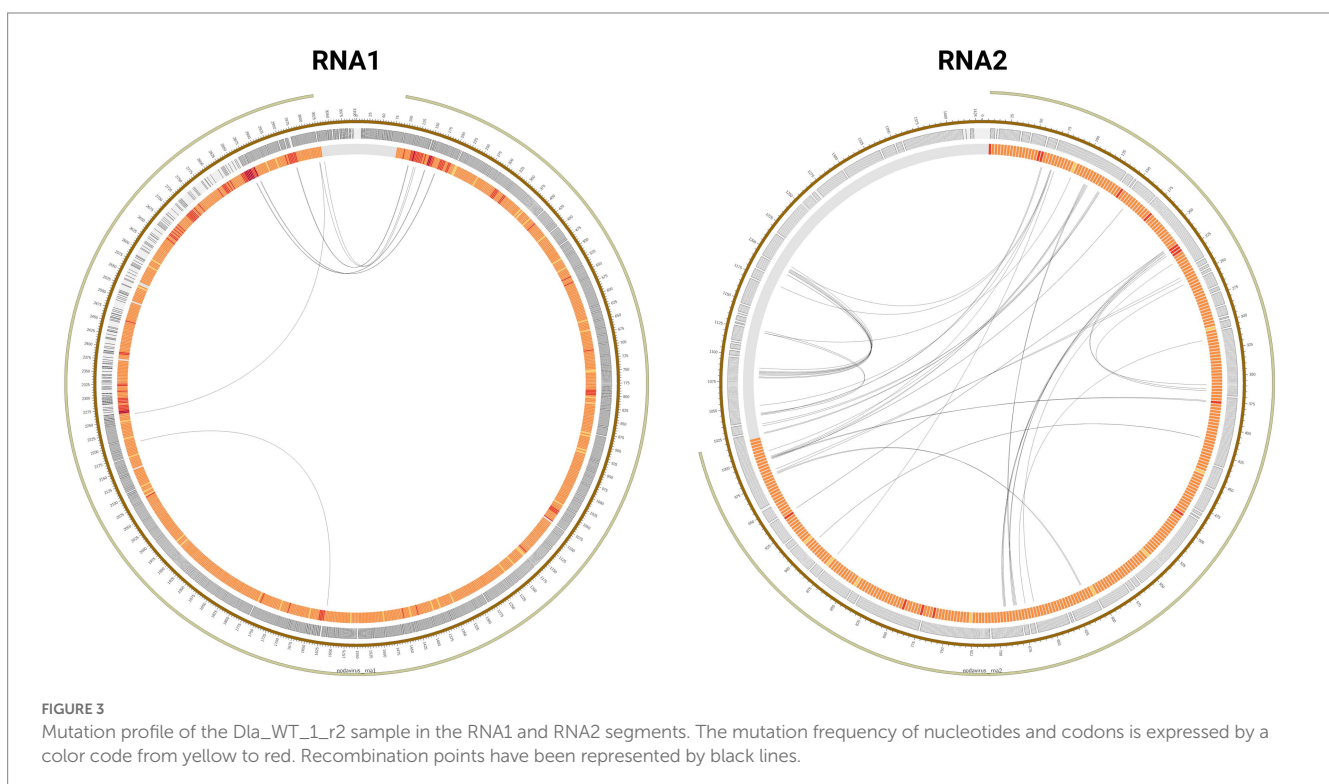
### 3.4. Genetic heterogeneity of mutant spectra in sea bass

We evaluated the heterogeneity of the viral samples by reconstructing haplotypes and estimating the normalized Shannon index for each sample. Focusing on RNA1 segment, rDI965 quasispecies presented more haplotypes with a greater variety of mutations at 5 dpi (0–8 haplotypes per sample at 1 dpi and 6–16 haplotypes per sample at 5 dpi), constituting more complex and dynamic networks. However, the Shannon index did not vary significantly (0–0.23 for rDI965 at 1 dpi and 0.10–0.32 for rDI965 at 5 dpi) (Table 2; Supplementary material S3). This was because the dominant haplotypes exhibited similar abundance in the quasispecies

in the 5 dpi samples (86–94%) as in the 1 dpi samples (90–99%) (Supplementary materials S7, S8). Mut270DI965 quasispecies on the first day of infection were more heterogeneous (8–13 haplotypes per sample, and Shannon index of 0.11–0.31). In addition, non-dominant haplotypes of relative abundance (8–27%) were detected in these samples. However, the heterogeneity in the quasispecies of both viruses was similar at 5 dpi (Table 2; Supplementary materials S3, S7, S8).

Regarding the RNA2 segment, important differences in the heterogeneity of the samples according to their virulence and time of infection were observed. In rDI965 samples, genetic heterogeneity was very low (3–4 haplotypes per sample, and Shannon index of 0.01–0.08). At 5 dpi, QuasiFlow did not detect enough variability to reconstruct haplotypes for each quasispecies (Table 2; Supplementary material S3). As shown in Figure 4 and Supplementary material S8, Mut270DI965 was more genetically heterogeneous in sea bass. The rDI965 quasispecies at 1 dpi were characterized by a few haplotypes, of which the dominant haplotype constituted 99% of the sequences. By contrast, Mut270DI965 quasispecies contained a greater number of haplotypes (10–18). However, it is noteworthy that the haplotypes in the Mut270DI965 samples were characterized by few mutations and very low relative abundance, except for sample DI\_Mut\_r1, where one haplotype with a frequency above 20% was recorded (Supplementary material S7). On the other hand, a decrease in heterogeneity in samples collected at 5 dpi (0–13 haplotypes per sample and 0–0.06 Shannon index) was also observed. Thus, a decrease in haplotype diversity was observed with the course of infection for both viruses, although less pronounced for the low virulent mutant (Table 2; Supplementary material S3).

In addition, rare haplotypes containing a considerable number of mutations were detected in several quasispecies regardless of its virulence, suggesting that they may have appeared as a result of a hypermutation phenomenon (Supplementary material S7).





98–99% of the isolated sequences. In contrast, samples at 5 dpi had slightly fewer haplotypes, but dominant haplotypes were less abundant (69–96%) and coexisted with relatively abundant haplotypes (3–30%) (Supplementary material S7). There were no significant differences with rDI965 samples in sea bass. However, rDI965 RNA2 quasiespecies in sea bream were more heterogeneous than those in sea bass, containing a greater number and abundance of haplotypes, especially at 5 dpi (Table 2; Supplementary materials S3, S7, S8).

The genetic characteristics of the quasiespecies recorded in sea bream and sea bass are summarized in Figure 6.

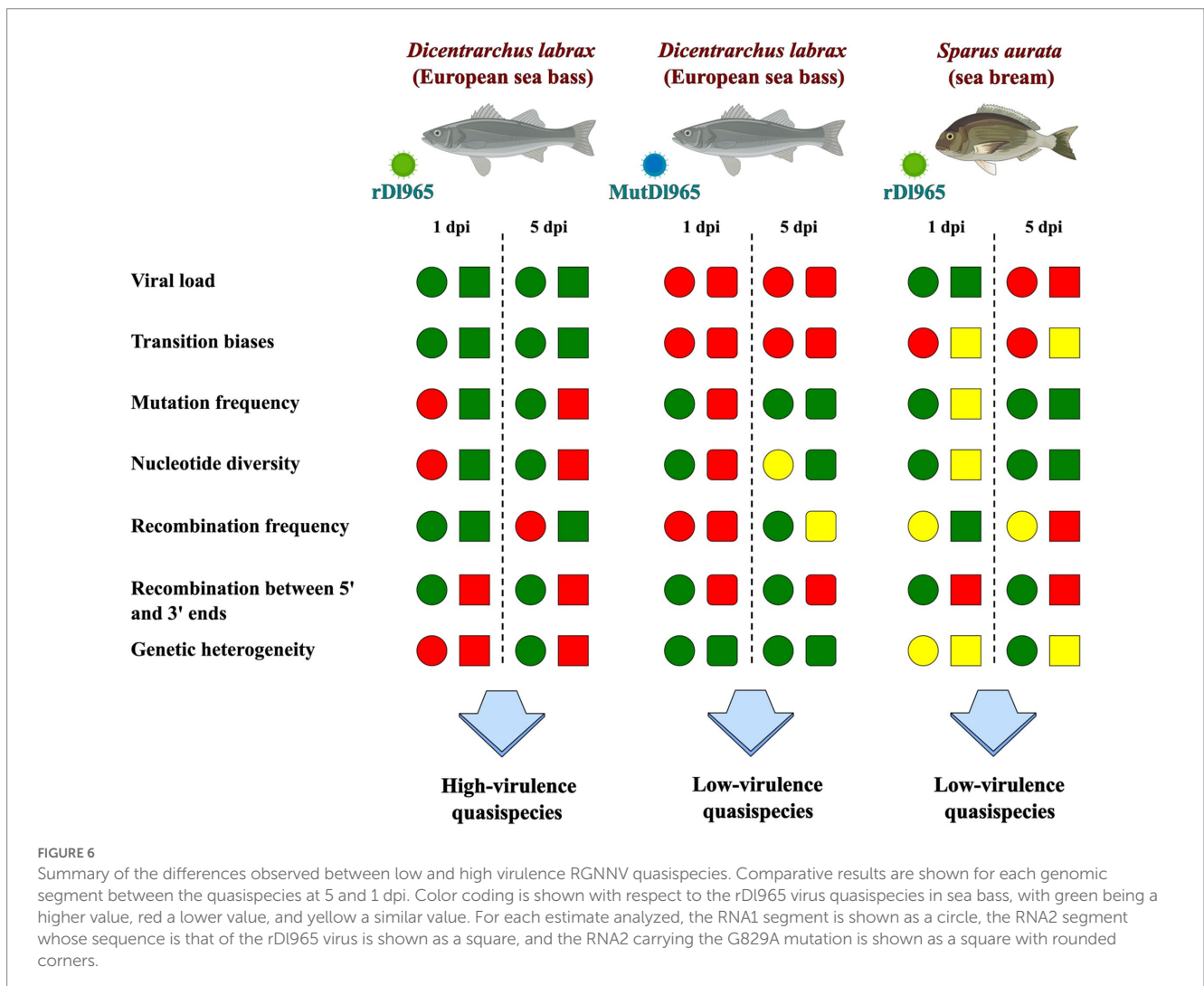
### 3.6. Multivariate analysis of virulent and non-virulent RGNNV infections in sea bass and sea bream

Comparative statistical analysis was carried out with the QuasiComparer workflow. We tested significant variations in the structure and variability of the NNV quasiespecies analyzed. A principal component analysis (PCA) considering all samples analyzed was performed for RNA1 and RNA2 segments together and separately (Figure 7). A total of 11 variables were included, such as Ts/Tv ratio,

Shannon index, transitions, transversions, ORF mutation frequency, SNPs or recombination events (Supplementary material S9). The genetic variables used to describe each sample in the PCA were defined in each dimension of the two-dimensional space.

We first performed the PCA by combining the two genomic segments. Almost all of the RNA1 sequences in the samples were grouped into two clusters, separate from the RNA2 sequences. Only two RNA1 samples were grouped with the RNA2 samples in the cluster. Samples isolated from different hosts were mixed. The RNA2 sequences were grouped into a single cluster. Mutation and recombination frequencies, as well as nucleotide diversity, were the most defining variables of this cluster. Thus, these variables were in RNA2 considerably different than in RNA1 in the RGNNV quasiespecies (Supplementary material S9).

We then performed two PCAs, one for each segment. PCA representations for RNA1 and RNA2 segments did not show well-defined clustering according to the features selected to classify each sample (host, dpi and virus). Samples grouped into three clusters (Figure 7). Cluster 1 comprised all rDI965 samples in sea bass, and was recorded for both viral segments. In both segments, no significant differences were observed between virulent quasiespecies of RGNNV in sea bass at 1 and 5 dpi. All Mut270DI965 sea bass samples and rDI965 in



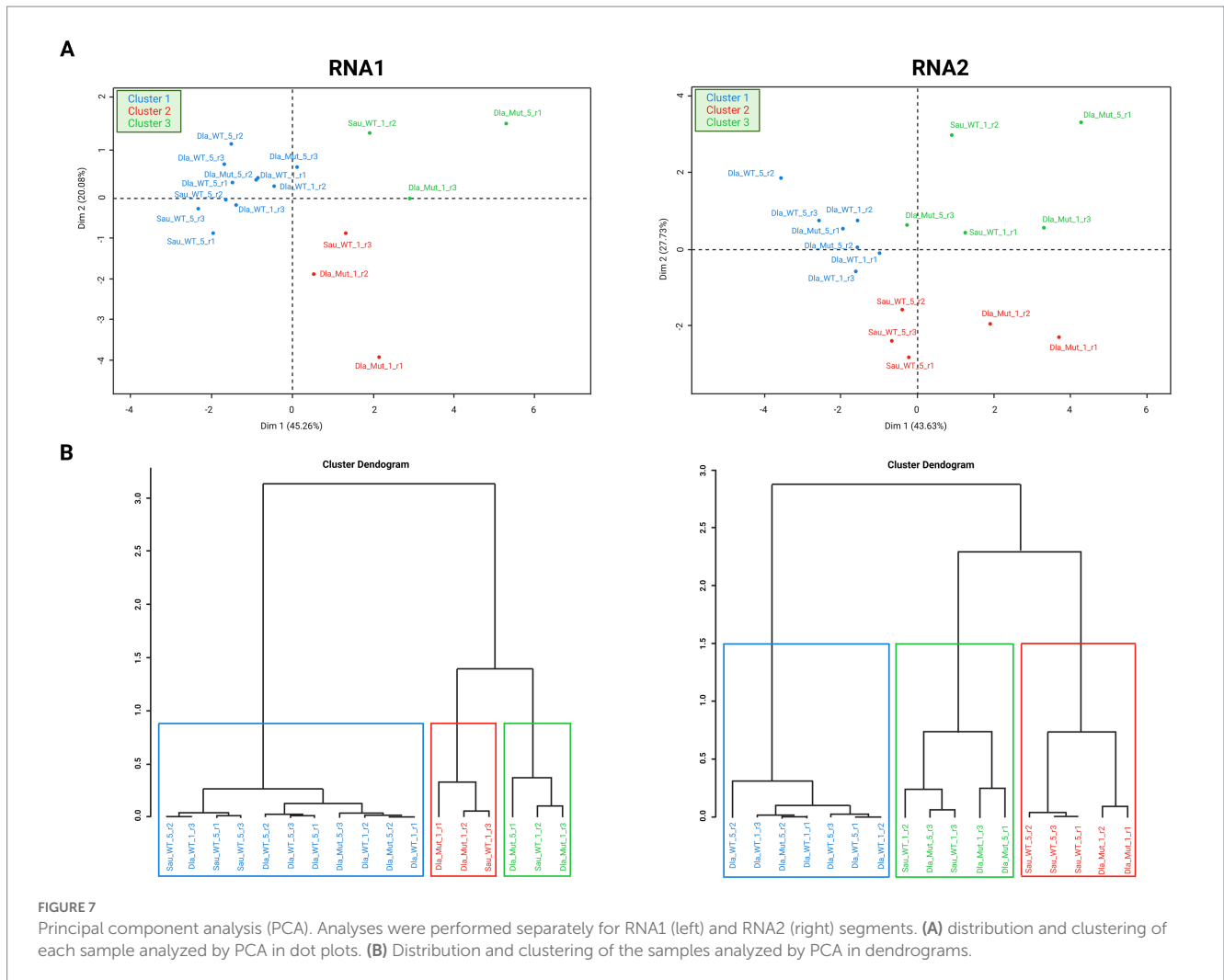


**FIGURE 7** Principal component analysis (PCA). Analyses were performed separately for RNA1 (left) and RNA2 (right) segments. **(A)** distribution and clustering of each sample analyzed by PCA in dot plots. **(B)** Distribution and clustering of the samples analyzed by PCA in dendrograms.

sea bream samples were grouped in two clusters (2 and 3) and separated from rDI965 quaspecies in sea bass (Cluster 1). Only two Mut270DI965 quaspecies were also included in RNA2 Cluster 1, and five were included in RNA1 Cluster 1 (two samples of Mut270DI965 from sea bass and three samples of rDI965 from sea bream). These results suggest that Mut270DI965 quaspecies in sea bass are more similar to rDI965 quaspecies in sea bream (low virulent) than to rDI965 quaspecies infecting sea bass (highly virulent). PCA analysis showed that the RNA2 of all rDI965 samples in sea bream at 1 dpi are significantly different from those detected at 5 dpi. These results contrast with those observed for RNA1 quaspecies.

Examining the distribution of the variables along the PCA axes, we found that the most important variable characterizing cluster 1 was the Ts/Tv ratio. In addition, the number of recombination events and the recombination frequency were also relevant in the PCA analysis of the RNA2 segment (Supplementary material S9).

## 4. Discussion

The role of amino acid at position 270 within the RGNNV capsid protein as a virulence determinant to sea bass has been recently shown. A non-synonymous mutation at this position (G829A), which replaces serine by asparagine (Ser270Asp), causes a decrease in

virulence to sea bass (Moreno et al., 2019). In RNA viruses, one or a few substitutions can alter adaptation and pathogenesis (Domingo et al., 2006). In the present study, we analyze how this mutation affects the structure and evolution of viral quaspecies *in vivo*.

The number of RNA1 and RNA2 copies in brain of sea bass and sea bream was quantified by absolute RT-qPCR at 1 and 5 dpi. The number of viral genome copies is higher in RGNNV-infected sea bass (highly virulent phenotype) than in Mut270DI965-sea bass (low virulent phenotype). These results suggest a positive correlation between viral load and virulence of NNV. However, the virulence of a virus is not necessary associated with replicating capacity and survival ability, i.e., its viral fitness (Domingo et al., 2008). The correlation between virulence and fitness may depend on complex virus-host interactions, as well as between coexisting variants in the host (Furió et al., 2012). At 1 dpi, the viral load in sea bream did not vary significantly compared to RNA levels detected in sea bass. However, at 5 dpi, it was observed that the viral load in sea bream was much lower than in sea bass. RGNNV infection in sea bream is asymptomatic, or generates mild symptoms, with no or very low mortality rate in juveniles (Castric et al., 2001; Valero et al., 2015), due to an efficient immune response (Poisa-Beiro et al., 2008; Pereiro et al., 2023).

In this work we analyze the genetics of RGNNV focusing on each genomic segment separately. Although there was a downward trend

in the RNA1 segment, there was no statistically significant difference in the estimated viral load in the RNA1 and RNA2 segments. In RNNV, there is a modulation in the replication of genomic segments that determines the load of each segment throughout the infectious cycle (Eckerle and Ball, 2002; Lindenbach et al., 2002; Souto et al., 2018). However, despite the similarities in the viral load, they had important differences in genetic variability between two segments. Focusing on rDI965 sea bass samples, the results suggest that the variation and diversification of each genomic segment is different in quasispecies throughout the infection. This finding was corroborated by PCA analyses performed with both segments. In segmented viruses, each segment undergoes a different genetic selection and diversification, allowing studying the evolutionary history of each segment independently (Rambaut et al., 2008; Freire et al., 2015). In our samples, RNA1 diversification was continuous along the infection in sea bass during the first 5 days. In contrast, RNA2 tended toward homogeneity over time. These current findings contrast with evolutionary analyses reporting that RGNV genome undergoes strong purifying selection pressure. However, they did show that the rate of evolution in the RNA1 was significantly higher than in the RNA2 segment (Panzarin et al., 2012).

Sequence analyses revealed that both genomic segments showed high genetic variability. Low-frequency mutations can be detected thanks to the in-depth assessment of the population structure and complexity of viral quasispecies enabled by NGS bioinformatics analysis tools (Pérez-Losada et al., 2020). However, NGS produces millions of error-prone short reads, generating artifacts from sequencing errors that may not be distinguishable from real mutations, especially low-frequency ones (Gregori et al., 2014, 2016; Knyazev et al., 2020). QuasiFlow performs a stringent filtering process on raw NGS reads that removes reads with sequence changes caused by artificial mutations, providing reliable detection of low-frequency genetic variations and ensuring the reliability of downstream analyses (Seoane et al., 2022).

In this report we suggest that changes in the genetic structure of *in vivo* quasispecies of a nodavirus may underlie differences in host virulence. Previously, different types of RGNV quasispecies have been shown to influence immunopathogenesis in a host undergoing persistent infection. These quasispecies possessed different characteristics, including localization within the host, infectivity or suppression of host immunity (Chen et al., 2020). Changes in genetic heterogeneity can dramatically affect virulence in a viral population (Vignuzzi et al., 2006). In this regard, we show that a single point mutation in the consensus sequence of the RNA2 segment, which encodes the capsid protein, caused a significant change in the quasispecies, affecting the virulence of the virus.

Focusing on the RNA2 segment, low virulent Mut270DI965 virus generated a more complex and genetically heterogeneous quasispecies. These data are surprising, given that a genetically homogeneous quasispecies may be more vulnerable and fail to overcome selection pressure. The generation of highly variable quasispecies allows viruses to adapt to different environments (Domingo et al., 2012; Domingo and Perales, 2019; Donohue et al., 2019; Delgado et al., 2021). A larger reservoir of mutations and haplotypes in a quasispecies favors not only host adaptation but can generate new phenotypes that positively affect virulence (Moreno et al., 2017). Previously, a mutant poliovirus with higher copy fidelity was reported to generate a more homogeneous quasispecies than the wild-type virus, resulting in the loss of its ability

to infect the central nervous system in mice (Pfeiffer and Kirkegaard, 2005; Vignuzzi et al., 2006). In Chikungunya virus (CHIKV), induction of high-fidelity mutations produced more diverse and virulent virus populations, whereas low-fidelity mutations generated less diverse populations that produce attenuated disease (Riemersma et al., 2019).

Despite higher haplotype diversity in the low-virulence virus populations, a tendency towards homogeneity was still detected, as revealed by a normalized Shannon index below 0.5. More haplotypes emerged in the low virulent quasispecies, although the frequency of the dominant haplotype did not change significantly compared to the virulent populations. Only in the Dla\_Mut\_1\_r1 sample a considerable increase in heterogeneity was detected, as a second haplotype emerged with a relatively high frequency (27%). As it has been described for the virulent virus samples, although with less intensity, this trend toward homogeneity increased at 5 dpi. The evolutionary history of a quasispecies is determined not by the characteristics of the fittest variant or master sequence, but by the set of variants that make up the mutant spectrum (Domingo et al., 2006; Domingo, 2016). Selection favors those genotypes with a faster replication rate, which also implies the production of new variants with lower fitness (Wilke et al., 2001). It should be noted that the samples collected at 1 and 5 dpi belong to different individuals. Therefore, to understand the evolution of RGNV quasispecies in a host, it would be necessary to investigate it in the same specimen during the course of the infection.

Virus-host interactions must be considered when determining the fate of a viral population. Changes in genetic heterogeneity are not only generated by disparity in the degree of genetic diversity, but can also be caused by differences in genomic patterns. Serial passaging assays in cell culture with an attenuated strain of mumps virus showed that the significant decrease in its neurovirulence came from changes in the proportion of mutations. Depending on the genome site, increases and decreases in the genetic heterogeneity of the attenuated quasispecies were found (Sauder et al., 2006). It has been reported that the pathogenesis of Newcastle disease virus (NDV) can be modulated by the proportion of avirulent and virulent genomes coexisting within the quasispecies and their interactions (Meng et al., 2016). These changes may result in purifying selection in the coding regions of virulent genotypes, affecting genetic diversity in this region (Jadhav et al., 2020).

Changes in virulence were associated with variations in the entire quasispecies, not only in the RNA2 segment. In RNA1, significant variations in recombination and mutation frequencies were detected in Mut270DI965 samples with respect to rDI965 samples. Furthermore, in the samples at 1 dpi we found that in the Mut270DI965 populations the nucleotide and haplotype diversity was higher. Therefore, our results suggest that the G829A mutation in RNA2 may affect the evolution of the viral quasispecies in the RNA1 segment. In segmented viruses, although each segment exhibits specific variability, the interaction between them influences their evolution (Pontremoli et al., 2018).

The properties of rDI965 quasispecies were evaluated in sea bream, a host less susceptible to RGNV. PCA analysis revealed that rDI965 populations isolated from sea bream were more closely related to the low virulent Mut270DI965-sea bass quasispecies than to the high virulent rDI965-sea bass quasispecies, especially with respect to the RNA2 segment. These results suggest that the genetic variability and evolution of a mutant spectrum may be primarily associated with

its virulence. Similarities existed between quasispecies inhabiting environments exposed to different selection pressures. In Mut270D1965 quasispecies, the Ser270Asp mutation may alter the interaction of the capsid protein with the cellular receptor (Moreno et al., 2019), which could constitute a bottleneck leading to quasispecies restriction, since it would impair RGNNV infection. Bottlenecks can abruptly change the structure and variability of a viral population (Pfeiffer and Kirkegaard, 2005; Cortey et al., 2018; Kadoya et al., 2020), establishing a founder effect that can lead to increased genetic diversity within quasispecies. This hypothesis could explain the increase in genetic variability and diversity in mutant virus populations at 1 dpi. The transcription of genes related to the innate immune response induced by Mut270D1965 is lower than that triggered by the wild-type virus (Moreno et al., 2019). This may result in weaker immune-mediated selection pressure and lead to greater diversification of viral populations. However, in sea bream, RGNNV infection generates a strong immune response (Pereiro et al., 2023). Sea bream is considered a natural reservoir of NNV (Castric et al., 2001; Chaves-Pozo et al., 2012; Valero et al., 2015). Nodavirus quasispecies may show different characteristics in healthy hosts than in hosts undergoing severe acute infection (Chen et al., 2020). This means that RGNNV populations present in potentially resistant hosts could develop their mutant clouds under strong immune-mediated pressure, acquiring different characteristics than if they were in a host susceptible to acute infection. Similarly, it would be desirable to analyze a highly virulent isolate for sea bream, in order to compare the quasispecies of virulent isolates of NNV between the two hosts.

Recombination events were very frequent in both segments in all samples analyzed. The frequency of recombination in the RNA1 sequence was considerably higher than the mutation frequency. Our results suggest the importance of recombination in the origin of genetic variability and the constitution of quasispecies throughout host infection. This is one of the first studies addressing the analysis of genetic material exchange events in NNV at an intrahost level. In NNV, genetic exchange and reassortment between viral species have been frequently described (Toffolo et al., 2007; Panzarin et al., 2012, 2014; Souto et al., 2015a; Toffan et al., 2017; Ariff et al., 2019; Volpe et al., 2020). However, the effects that recombinant haplotypes within an RGNNV quasispecies may have on pathogenesis are still unknown.

Cumulative recombination events were observed between the 5' and 3' ends of the RNA1 segment in all samples analyzed. These patterns of recombination events in the RNA1 segment could suggest the synthesis of circular RNAs (circRNAs) in RGNNV. CircRNAs can be generated through backsplicing (Choudhary et al., 2021; Tan et al., 2021), a process that has not yet been described in NNV. The generation of circRNAs is present in both, DNA and RNA viruses (Zhang et al., 2022). In herpesviruses (double-stranded DNA viruses), the generation of circRNAs has been observed in response to activation of the lytic cycle of infection. These molecules may participate in the regulation of processes such as cell proliferation or host innate immune response (Tagawa et al., 2018; Tan et al., 2021). They have only been described in some negative-stranded RNA viruses encoding viral circRNAs. The synthesis of circRNA molecules has been described in sarbecoviruses (Cai et al., 2021), and it is suggested that they may be involved in the generation of homologous recombinants (Hassanin et al., 2022). CircRNAs has been discovered in a fish dsRNA virus, grass carp reovirus (GCRV). Some of these molecules were formed by alternative splicing, and intervened by

suppressing GCRV replication (Pan et al., 2021). However, we cannot confirm, beyond the results obtained by bioinformatics analysis, the generation of circRNAs in RGNNV. The role that this process may play in viral pathogenesis is also undetermined. Further work on the detection and functional characterization of circRNAs is needed in future studies.

## Data availability statement

The data presented in the study are deposited in the SRA repository, accession number PRJNA942601, and can be found at: <https://www.ncbi.nlm.nih.gov/sra/PRJNA942601>.

## Ethics statement

The animal study was reviewed and approved by Bioethics Committee of Junta de Andalucía (number: 09/08/2019/136).

## Author contributions

AG-P, JB, EG-R, MA, and LD-M: conceptualization and design of the study. LD-M, PM, and SO-D-C: investigation and formal analysis. LD-M and SO-D-C: bioinformatics and statistical analysis. SO-D-C and AG-P: writing. All authors contributed to manuscript revisions, read, edition, and approved the submitted version.

## Funding

This study has been supported by the project PID2020-115954RB-I00/AEI/10.13039/501100011033 (Spanish Government). JB and AG-P are grateful to the Plan Propio of the University of Malaga.

## Conflict of interest

The authors declare that the research was conducted in the absence of any commercial or financial relationships that could be construed as a potential conflict of interest.

## Publisher's note

All claims expressed in this article are solely those of the authors and do not necessarily represent those of their affiliated organizations, or those of the publisher, the editors and the reviewers. Any product that may be evaluated in this article, or claim that may be made by its manufacturer, is not guaranteed or endorsed by the publisher.

## Supplementary material

The Supplementary material for this article can be found online at: <https://www.frontiersin.org/articles/10.3389/fmicb.2023.1182695/full#supplementary-material>

## References

- Ariff, N., Abdullah, A., Azmai, M. N. A., Musa, N., and Zainathan, S. C. (2019). Risk factors associated with viral nervous necrosis in hybrid groupers in Malaysia and the high similarity of its causative agent nervous necrosis virus to reassortant red-spotted grouper nervous necrosis virus/striped jack nervous necrosis virus strains. *Vet World* 12, 1273–1284. doi: 10.14202/vetworld.2019.1273-1284
- Bandin, I., and Souto, S. (2020). Betanodavirus and VER disease: a 30-year research review. *Pathogens* 9:106. doi: 10.3390/pathogens9020106
- Biasini, L., Berto, P., Abbadi, M., Buratin, A., Toson, M., Marsella, A., et al. (2022). Pathogenicity of different Betanodavirus RGNNV/SJNNV Reassortant strains in European Sea bass. *Pathogens* 11:458. doi: 10.3390/pathogens11040458
- Cai, Z., Lu, C., He, J., Liu, L., Zou, Y., Zhang, Z., et al. (2021). Identification and characterization of circRNAs encoded by MERS-CoV, SARS-CoV-1 and SARS-CoV-2. *Brief. Bioinform.* 22, 1297–1308. doi: 10.1093/bib/bbaa334
- Carballo, C., Garcia-Rosado, E., Borrego, J. J., and Alonso, M. C. (2016). SJNNV down-regulates RGNNV replication in European sea bass by the induction of the type I interferon system. *Vet. Res.* 47:6. doi: 10.1186/s13567-015-0304-y
- Castric, J., Thiéry, R., Jeffroy, J., de Kinkelin, P., and Raymond, J. (2001). Sea bream *Sparus aurata*, an asymptomatic contagious fish host for nodavirus. *Dis. Aquat. Org.* 47, 33–38. doi: 10.3354/dao047033
- Chaves-Pozo, E., Guardiola, F. A., Meseguer, J., Esteban, M. A., and Cuesta, A. (2012). Nodavirus infection induces a great innate cell-mediated cytotoxic activity in resistant, gilthead seabream, and susceptible, European sea bass, teleost fish. *Fish Shellfish Immunol.* 33, 1159–1166. doi: 10.1016/j.fsi.2012.09.002
- Chen, Y.-M., Tan, C. S., Wang, T.-Y., Hwong, C.-L., and Chen, T.-Y. (2020). Characterization of betanodavirus quasispecies influences on the subcellular localization and expression of tumor necrosis factor (TNF). *Fish Shellfish Immunol.* 103, 332–341. doi: 10.1016/j.fsi.2020.05.031
- Chen, N.-C., Yoshimura, M., Guan, H.-H., Wang, T.-Y., Misumi, Y., Lin, C.-C., et al. (2015). Crystal structures of a piscine Betanodavirus: mechanisms of capsid assembly and viral infection. *PLoS Pathog.* 11:e1005203. doi: 10.1371/journal.ppat.1005203
- Choudhary, A., Madhbagat, P., Sreepadmanabh, M., Bhardwaj, V., and Chande, A. (2021). Circular RNA as an additional player in the conflicts between the host and the virus. *Front. Immunol.* 12:602006. doi: 10.3389/fimmu.2021.602006
- Cortey, M., Arocena, G., Pileri, E., Martín-Valls, G., and Mateu, E. (2018). Bottlenecks in the transmission of porcine reproductive and respiratory syndrome virus (PRRSV1) to naïve pigs and the quasi-species variation of the virus during infection in vaccinated pigs. *Vet. Res.* 49:107. doi: 10.1186/s13567-018-0603-1
- Delgado, S., Perales, C., García-Crespo, C., Soria, M. E., Gallego, I., de Ávila, A. I., et al. (2021). A two-level, intramutant spectrum haplotype profile of hepatitis C virus revealed by self-organized maps. *Microbiol. Spectrum* 9:e0145921. doi: 10.1128/Spectrum.01459-21
- Doan, Q. K., Vandeputte, M., Chatain, B., Morin, T., and Allal, F. (2017). Viral encephalopathy and retinopathy in aquaculture: a review. *J. Fish Dis.* 40, 717–742. doi: 10.1111/jfd.12541
- Domingo, E. (2016). *Virus as populations: Composition, complexity, dynamics, and biological implications*. Cambridge, MA: Elsevier/Academic Press.
- Domingo, E., Escarmís, C., Menéndez-Arias, L., Perales, C., Herrera, M., Novella, I. S., et al. (2008). “Viral Quasispecies: Dynamics, Interactions, and Pathogenesis,” *Origin and Evolution of Viruses*. eds. E. Domingo, C. R. Parrish and J. J. Holland (Amsterdam, NL: Elsevier), 87–118.
- Domingo, E., Martín, V., Perales, C., Grande-Pérez, A., García-Arriaza, J., and Arias, A. (2006). Viruses as Quasispecies: biological implications. *Curr. Top Microbiol. Immunol.* 299, 51–82. doi: 10.1007/3-540-26397-7\_3
- Domingo, E., and Perales, C. (2019). Viral quasispecies. *PLoS Genetics* 15:e1008271. doi: 10.1371/journal.pgen.1008271
- Domingo, E., Sheldon, J., and Perales, C. (2012). Viral Quasispecies Evolution. *Microbiol. Mol. Biol. Rev.* 76, 159–216. doi: 10.1128/MMBR.05023-11
- Donohue, R. C., Pfaller, C. K., and Cattaneo, R. (2019). Cyclical adaptation of measles virus quasispecies to epithelial and lymphocytic cells: to V, or not to V. *PLoS Pathog.* 15:e1007605. doi: 10.1371/journal.ppat.1007605
- Eckerle, L. D., and Ball, L. A. (2002). Replication of the RNA segments of a bipartite viral genome is coordinated by a transactivating subgenomic RNA. *Virology* 296, 165–176. doi: 10.1006/viro.2002.1377
- Freire, C. C. M., Iammarino, A., Soumaré, P. O. L., Faye, O., Sall, A. A., and Zanotto, P. M. A. (2015). Reassortment and distinct evolutionary dynamics of Rift Valley fever virus genomic segments. *Sci. Rep.* 5:11353. doi: 10.1038/srep11353
- Furió, V., Garijo, R., Durán, M., Moya, A., Bell, J. C., and Sanjuán, R. (2012). Relationship between within-host fitness and virulence in the vesicular stomatitis virus: correlation with partial decoupling. *J. Virol.* 86, 12228–12236. doi: 10.1128/JVI.00755-12
- Gregori, J., Perales, C., Rodríguez-Frias, F., Esteban, J. I., Quer, J., and Domingo, E. (2016). Viral quasispecies complexity measures. *Virology* 493, 227–237. doi: 10.1016/j.virol.2016.03.017
- Gregori, J., Salicrú, M., Domingo, E., Sanchez, A., Esteban, J. I., Rodríguez-Frias, F., et al. (2014). Inference with viral quasispecies diversity indices: clonal and NGS approaches. *Bioinformatics* 30, 1104–1111. doi: 10.1093/bioinformatics/btt768
- Hassanin, A., Rambaud, O., and Klein, D. (2022). Genomic bootstrap barcodes and their application to study the evolution of Sarbecoviruses. *Viruses* 14:440. doi: 10.3390/v14020440
- Hick, P., Tweedie, A., and Whittington, R. (2010). Preparation of fish tissues for optimal detection of betanodavirus. *Aquaculture* 310, 20–26. doi: 10.1016/j.aquaculture.2010.10.005
- Iwamoto, T., Mise, K., Mori, K., Arimoto, M., Nakai, T., and Okuno, T. (2001). Establishment of an infectious RNA transcription system for striped jack nervous necrosis virus, the type species of the betanodaviruses. *J. Gen. Virol.* 82, 2653–2662. doi: 10.1099/0022-1317-82-11-2653
- Jadhav, A., Zhao, L., Liu, W., Ding, C., Nair, V., Ramos-Onsins, S. E., et al. (2020). Genomic Diversity and Evolution of Quasispecies in Newcastle Disease Virus Infections. *Viruses* 12:1305. doi: 10.3390/v12111305
- Kadoya, S.-S., Urayama, S.-I., Nunoura, T., Hirai, M., Takaki, Y., Kitajima, M., et al. (2020). Bottleneck size-dependent changes in the genetic diversity and specific growth rate of a rotavirus a strain. *J. Virol.* 94, e02083–e02019. doi: 10.1128/JVI.02083-19
- Kara, H. M., Chaoui, L., Derbal, F., Zaidi, R., de Boissésion, C., Baud, M., et al. (2014). Betanodavirus-associated mortalities of adult wild groupers *Epinephelus marginatus* (Lowe) and *Epinephelus costae* (Steindachner) in Algeria. *J. Fish Dis.* 37, 273–278. doi: 10.1111/jfd.12020
- Knyazev, S., Hughes, L., Skums, P., and Zelikovsky, A. (2020). Epidemiological data analysis of viral quasispecies in the next-generation sequencing era. *Brief. Bioinform.* 22, 96–108. doi: 10.1093/bib/bbaa101
- Le Breton, A., Grisez, L., Sweetman, J., and Ollevier, F. (1997). Viral nervous necrosis (VNN) associated with mass mortalities in cage-reared sea bass, *Dicentrarchus labrax* (L.). *J. Fish Dis.* 20, 145–151. doi: 10.1046/j.1365-2761.1997.00284.x
- Lindenbach, B. D., Sgro, J.-Y., and Ahlquist, P. (2002). Long-distance base pairing in flock house virus RNA1 regulates subgenomic RNA3 synthesis and RNA2 replication. *J. Virol.* 76, 3905–3919. doi: 10.1128/jvi.76.8.3905-3919.2002
- Lopez-Jimena, B., Alonso, M. D. C., Thompson, K. D., Adams, A., Infante, C., Castro, D., et al. (2011). Tissue distribution of red spotted grouper nervous necrosis virus (RGNNV) genome in experimentally infected juvenile European seabass (*Dicentrarchus labrax*). *Vet. Microbiol.* 154, 86–95. doi: 10.1016/j.vetmic.2011.06.029
- Meng, C., Qiu, X., Yu, S., Li, C., Sun, Y., Chen, Z., et al. (2016). Evolution of Newcastle Disease Virus Quasispecies Diversity and Enhanced Virulence after Passage through Chicken Air Sacs. *J. Virol.* 90, 2052–2063. doi: 10.1128/JVI.01801-15
- Moreno, E., Gallego, I., Gregori, J., Lucía-Sanz, A., Soria, M. E., Castro, V., et al. (2017). Internal disequilibria and phenotypic diversification during replication of hepatitis C virus in a noncoevolving cellular environment. *J. Virol.* 91:16. doi: 10.1128/JVI.02505-16
- Moreno, P., Garcia-Rosado, E., Borrego, J. J., and Alonso, M. C. (2016). Genetic characterization and transcription analyses of the European sea bass (*Dicentrarchus labrax*) isg15 gene. *Fish Shellfish Immunol.* 55, 642–646. doi: 10.1016/j.fsi.2016.06.043
- Moreno, P., Souto, S., Leiva-Rebollo, R., Borrego, J. J., Bandin, I., and Alonso, M. C. (2019). Capsid amino acids at positions 247 and 270 are involved in the virulence of betanodaviruses to European sea bass. *Sci. Rep.* 9:14068. doi: 10.1038/s41598-019-50622-1
- Munday, B. L., Kwang, J., and Moody, N. (2002). Betanodavirus infections of teleost fish: a review. *J. Fish Dis.* 25, 127–142. doi: 10.1046/j.1365-2761.2002.00350.x
- Nishizawa, T., Furuhashi, M., Nagai, T., Nakai, T., and Muroga, K. (1997). Genomic classification of fish nodaviruses by molecular phylogenetic analysis of the coat protein gene. *Appl. Environ. Microbiol.* 63, 1633–1636. doi: 10.1128/aem.63.4.1633-1636.1997
- Olveira, J. G., Souto, S., Dopazo, C. P., Thiéry, R., Barja, J. L., and Bandin, I. (2009). Comparative analysis of both genomic segments of betanodaviruses isolated from epizootic outbreaks in farmed fish species provides evidence for genetic reassortment. *J. Gen. Virol.* 90, 2940–2951. doi: 10.1099/vir.0.013912-0
- Pan, J., Zhang, X., Zhang, Y., Yan, B., Dai, K., Zhu, M., et al. (2021). Grass carp reovirus encoding circular RNAs with antiviral activity. *Aquaculture* 533:736135. doi: 10.1016/j.aquaculture.2020.736135
- Panzarin, V., Cappelozza, E., Mancin, M., Milani, A., Toffan, A., Terregino, C., et al. (2014). *In vitro* study of the replication capacity of the RGNNV and the SJNNV betanodavirus genotypes and their natural reassortants in response to temperature. *Vet. Res.* 45:56. doi: 10.1186/1297-9716-45-56
- Panzarin, V., Fusaro, A., Monne, I., Cappelozza, E., Patarnello, P., Bovo, G., et al. (2012). Molecular epidemiology and evolutionary dynamics of betanodavirus in southern Europe. *Infect. Genet. Evol.* 12, 63–70. doi: 10.1016/j.meegid.2011.10.007
- Panzarin, V., Toffan, A., Abbadi, M., Buratin, A., Mancin, M., Braaen, S., et al. (2016). Molecular basis for antigenic diversity of genus Betanodavirus. *PLoS One* 11:e0158814. doi: 10.1371/journal.pone.0158814

- Pereiro, P., Figueras, A., and Novoa, B. (2023). RNA-Seq analysis of juvenile gilthead sea bream (*Sparus aurata*) provides some clues regarding their resistance to the nodavirus RGNNV genotype. *Fish Shellfish Immunol.* 134:108588. doi: 10.1016/j.fsi.2023.108588
- Pérez-Losada, M., Arenas, M., Galán, J. C., Bracho, M. A., Hillung, J., García-González, N., et al. (2020). High-throughput sequencing (HTS) for the analysis of viral populations. *Infect. Genet. Evol.* 80:104208. doi: 10.1016/j.meegid.2020.104208
- Pérez-Sánchez, T., Mora-Sánchez, B., and Balcázar, J. L. (2018). Biological approaches for disease control in aquaculture: advantages, Limitations and Challenges. *Trends Microbiol.* 26, 896–903. doi: 10.1016/j.tim.2018.05.002
- Pfeiffer, J. K., and Kirkegaard, K. (2005). Increased fidelity reduces poliovirus fitness and virulence under selective pressure in mice. *PLoS Pathog.* 1:e11. doi: 10.1371/journal.ppat.0010011
- Poisa-Beiro, L., Dios, S., Montes, A., Aranguren, R., Figueras, A., and Novoa, B. (2008). Nodavirus increases the expression of mx and inflammatory cytokines in fish brain. *Mol. Immunol.* 45, 218–225. doi: 10.1016/j.molimm.2007.04.016
- Pontremoli, C., Forni, D., Cagliani, R., and Sironi, M. (2018). Analysis of Reptarenavirus genomes indicates different selective forces acting on the S and L segments and recent expansion of common genotypes. *Infect. Genet. Evol.* 64, 212–218. doi: 10.1016/j.meegid.2018.06.031
- Qin, Y., Liu, J., Liu, W., Shi, H., Jia, A., Lu, Y., et al. (2020). First isolation and identification of red-grouper nervous necrosis virus (RGNNV) from adult hybrid Hulong grouper (*Epinephelus fuscoguttatus* × *Epinephelus lanceolatus*) in China. *Aquaculture* 529:735662. doi: 10.1016/j.aquaculture.2020.735662
- Rambaut, A., Pybus, O. G., Nelson, M. I., Viboud, C., Taubenberger, J. K., and Holmes, E. C. (2008). The genomic and epidemiological dynamics of human influenza A virus. *Nature* 453, 615–619. doi: 10.1038/nature06945
- Reed, L. J., and Muench, H. (1938). A Simple Method of Estimating Fifty Per Cent Endpoints. *Am. J. Epidemiol.* 27, 493–497. doi: 10.1093/oxfordjournals.aje.a118408
- Riemersma, K. K., Steiner, C., Singapuri, A., and Coffey, L. L. (2019). Chikungunya virus Fidelity variants exhibit differential attenuation and population diversity in cell culture and adult mice. *J. Virol.* 93, e01606–e01618. doi: 10.1128/JVI.01606-18
- Sauder, C. J., Vandenburgh, K. M., Iskow, R. C., Malik, T., Carbone, K. M., and Rubin, S. A. (2006). Changes in mumps virus neurovirulence phenotype associated with quasispecies heterogeneity. *Virology* 350, 48–57. doi: 10.1016/j.virol.2006.01.035
- Seoane, P., Díaz-Martínez, L., Viguera, E., Claros, M. G., and Grande-Pérez, A. (2022). QuasiFlow: A bioinformatic tool for genetic variability analysis from next generation sequencing data. *bioRxiv*. doi: 10.1101/2022.04.05.487169
- Souto, S., Lopez-Jimena, B., Alonso, M. C., García-Rosado, E., and Bandín, I. (2015a). Experimental susceptibility of European sea bass and Senegalese sole to different betanodavirus isolates. *Vet. Microbiol.* 177, 53–61. doi: 10.1016/j.vetmic.2015.02.030
- Souto, S., Mérour, E., Biacchesi, S., Brémont, M., Oliveira, J. G., and Bandín, I. (2015b). *In vitro* and *in vivo* characterization of molecular determinants of virulence in reassortant betanodavirus. *J. Gen. Virol.* 96, 1287–1296. doi: 10.1099/vir.0.000064
- Souto, S., Oliveira, J. G., Dopazo, C. P., Borrego, J. J., and Bandín, I. (2018). Modification of betanodavirus virulence by substitutions in the 3' terminal region of RNA2. *J. Gen. Virol.* 99, 1210–1220. doi: 10.1099/jgv.0.001112
- Sugaya, T., Mori, K., Nishioka, T., Masuma, S., Oka, M., Mushiaka, K., et al. (2009). Genetic heterogeneity of betanodaviruses in juvenile production trials of Pacific bluefin tuna, *Thunnus orientalis* (Temminck & Schlegel). *J. Fish Dis.* 32, 815–824. doi: 10.1111/j.1365-2761.2009.01057.x
- Tagawa, T., Gao, S., Koparde, V. N., Gonzalez, M., Spouge, J. L., Serquiña, A. P., et al. (2018). Discovery of Kaposi's sarcoma herpesvirus-encoded circular RNAs and a human antiviral circular RNA. *Proc. Natl. Acad. Sci. U. S. A.* 115, 12805–12810. doi: 10.1073/pnas.1816183115
- Tan, K.-E., Ng, W. L., Marinov, G. K., Yu, K. H.-O., Tan, L. P., Liao, E. S., et al. (2021). Identification and characterization of a novel Epstein-Barr virus-encoded circular RNA from LMP-2 gene. *Sci. Rep.* 11:14392. doi: 10.1038/s41598-021-93781-w
- Thiéry, R., Cozien, J., de Boissésion, C., Kerbart-Boscher, S., and Névárez, L. (2004). Genomic classification of new betanodavirus isolates by phylogenetic analysis of the coat protein gene suggests a low host-fish species specificity. *J. Gen. Virol.* 85, 3079–3087. doi: 10.1099/vir.0.80264-0
- Toffan, A., Pascoli, F., Pretto, T., Panzarín, V., Abbadi, M., Buratin, A., et al. (2017). Viral nervous necrosis in gilthead sea bream (*Sparus aurata*) caused by reassortant betanodavirus RGNNV/SJNNV: an emerging threat for Mediterranean aquaculture. *Sci. Rep.* 7:46755. doi: 10.1038/srep46755
- Toffolo, V., Negrísolo, E., Maltese, C., Bovo, G., Belvedere, P., Colombo, L., et al. (2007). Phylogeny of betanodaviruses and molecular evolution of their RNA polymerase and coat proteins. *Mol. Phylogenet. Evol.* 43, 298–308. doi: 10.1016/j.ympev.2006.08.003
- Valero, Y., Arizcun, M., Esteban, M. Á., Bandín, I., Oliveira, J. G., Patel, S., et al. (2015). Nodavirus colonizes and replicates in the testis of gilthead seabream and European Sea bass modulating its immune and reproductive functions. *PLoS One* 10:e0145131. doi: 10.1371/journal.pone.0145131
- Vendramin, N., Toffan, A., Mancin, M., Cappelozza, E., Panzarín, V., Bovo, G., et al. (2014). Comparative pathogenicity study of ten different betanodavirus strains in experimentally infected European sea bass, *Dicentrarchus labrax* (L.). *J. Fish Dis.* 37, 371–383. doi: 10.1111/jfd.12117
- Vignuzzi, M., Stone, J. K., Arnold, J. J., Cameron, C. E., and Andino, R. (2006). Quasispecies diversity determines pathogenesis through cooperative interactions in a viral population. *Nature* 439, 344–348. doi: 10.1038/nature04388
- Volpe, E., Gustinelli, A., Caffara, M., Errani, F., Quaglio, F., Fioravanti, M. L., et al. (2020). Viral nervous necrosis outbreaks caused by the RGNNV/SJNNV reassortant betanodavirus in gilthead sea bream (*Sparus aurata*) and European sea bass (*Dicentrarchus labrax*). *Aquaculture* 523:735155. doi: 10.1016/j.aquaculture.2020.735155
- Wilke, C. O., Wang, J. L., Ofria, C., Lenski, R. E., and Adami, C. (2001). Evolution of digital organisms at high mutation rates leads to survival of the flattest. *Nature* 412, 331–333. doi: 10.1038/35085569
- Zhang, X., Liang, Z., Wang, C., Shen, Z., Sun, S., Gong, C., et al. (2022). Viral circular RNAs and their possible roles in virus-host interaction. *Front. Immunol.* 13:939768. doi: 10.3389/fimmu.2022.939768